American Journal of Applied and Industrial Chemistry
2026, Vol. 10, No. 1, pp. 1–11
https://doi.org/10.11648/j.ajaic.20261001.11

Research Article

Synthesis of Silver–3,5-dimethylphenol –Cyclodextrin Nanomaterials and pH-Dependent Characteristics of 3,5-Dimethylphenol –Cyclodextrin Inclusion Complexes

Narayanasamy Rajendiran[1, *], Ayyadurai Mani[1], Palanichamy Ramasamy[2], Sengamalai Senthilmurugan[3]

[1]Department of Chemistry, Annamalai University, Annamalai Nagar, India
[2]Molecular Biophysics Unit, Indian Institute of Science, Bangalore, India
[3]Department of Zoology, Annamalai University, Annamalai Nagar, India

Abstract

Absorption, emission, and time-resolved fluorescence maxima of 3,5-dimethylphenol (35DMP) were examined in various solvents, as well as in α-CD and β-CD solutions at pH ~2, pH ~7, and pH ~11. The corresponding nanomaterials were synthesized and characterized using SEM, DSC, FTIR, XRD, and ^{1}H NMR analyses. In CD solutions, the absorption and emission spectra of 35DMP are similar at pH ~2 and pH ~7 but differ at pH ~11. At higher β-CD concentrations, the spectral maxima and shapes are similar in all the pH, suggesting the formation of a same type of inclusion complex. But, α-CD shows distinct absorption and emission maxima at different pH values, indicating the formation of different inclusion. 35DMP is more deeply encapsulated in the nonpolar interior of β-CD than in α-CD, as reflected by the increase in fluorescence lifetime in the order: pH < α-CD < β-CD. The calculated HOMO–LUMO energy gap, total energy, free energy, enthalpy, entropy, dipole moment, and zero-point vibrational energy of the CD: 35DMPcomplex differed significantly from those of the isolated 35DMP, α-CD and β-CD molecules, and both the vertical and horizontal bond lengths between the methyl and hydroxy groups are smaller than the β-CD cavity size confirming the formation of an inclusion complex. SEM-EDX analysis confirmed the presence of silver in the nanomaterials. DSC thermograms of Ag: 35DMP: CD complexes show new thermal peaks distinct from those of pure 35DMP, α-CD, and β-CD. FTIR spectra of the nanomaterials indicate substantial decreases or absence of most characteristic peaks, confirming strong interactions between 35DMP, the CD cavity, and the silver nanoparticles.

Keywords

3,5-dimethylphenol, Cyclodextrin, Silver Nano, Inclusion Complex

1. Introduction

Cyclodextrins are known to accommodate guest molecules of diverse sizes [1-15], giving rise to various inclusion modes such as full encapsulation inside the cavity, partial penetration, or binding near the rim. CD complexation is well recognized

*Correspondence: Narayanasamy Rajendiran (drrajendiran1967@gmail.com)

Received: 11 March 2026; **Accepted:** 23 March 2026; **Published:** 10 April 2026

for modifying several physicochemical properties of guest molecules, including electronic absorption, fluorescence, phosphorescence, and ^{1}H NMR spectra, as well as acid–base equilibria and excited-state proton transfer processes. Organic compounds [16-25] often exhibit pronounced photophysical changes in response to variations in solvent polarity, pH, and the CD microenvironment. Substituted phenols, in particular, display distinct behavior under such conditions. Over the last two decades, our laboratory has investigated the excited-state acid–base properties of numerous fluorophores in both solvent and CD media [16-25]. In continuation of these efforts, we examined 3,5-dimethylphenol (35DMP) and its interactions with α-CD and β-CD, which serve as widely studied models for host–guest complexation. Because of the inherent challenges in accurately modeling solvation, theoretical calculations were restricted to gas-phase host–guest interactions.

In this study, we report: (i) the absorption and fluorescence spectral shifts and first excited singlet-state lifetimes of 35DMP in α-CD, β-CD, solvents of varying polarities, and at different pH values; (ii) the proton-transfer behavior of 35DMP in aqueous, α-CD, and β-CD media; (iii) the structure and geometry of the inclusion complexes based on PM3 molecular modeling; and (iv) the doping effects of 35DMP: CD complexes on silver nanomaterials, characterized using DSC, FTIR, ^{1}H NMR, and SEM techniques.

2. Materials and Methods

2.1. Preparation of CD Solution

The stock solution of 35DMP was prepared at a concentration of 2×10^{-2} mol dm^{-3}. Aliquots of 0.1 or 0.2 mL of this stock solution were transferred into 10 mL volumetric flasks. To each flask, varying concentrations of α-CD or β-CD solutions (0.2, 0.4, 0.6, 0.8, and 1.0×10^{-2} mol dm^{-3}) were added. The mixtures were then diluted to the mark with triply distilled water and thoroughly shaken. The final concentration of 35DMP in all prepared solutions was maintained at 4×10^{-4} mol dm^{-3}. All experiments were conducted at room temperature (298 K).

2.2. Synthesis of Ag: 35DMP: CD Nanomaterials

A 0.01 M solution of silver nitrate was prepared in 50 mL of deionized water and warmed at 50–60 ℃ for 30 minutes. Subsequently, 1–2 mL of 1% trisodium citrate solution (1 g in 100 mL deionized water) was added with vigorous stirring. The appearance of a pale-yellow coloration indicated the formation of silver nanoparticles [24-28].

CD (1 mmol) was dissolved in 40 mL of distilled water, and 35DMP (1 mmol) dissolved in 10 mL of ethanol was slowly added to the CD solution. The mixture was stirred at 50 ℃ for 2 hours using a magnetic stirrer. The freshly prepared silver nanoparticle solution was then added, and stirring continued for another 2 hours. This dilute mixture was gently heated at 40–50 ℃ until the volume was reduced to approximately 50%. The solution was refrigerated overnight at 5 ℃. The resulting Ag–35DMP–CD nanomaterial precipitate was collected by filtration and washed with small amounts of ethanol and water to remove any uncomplexed 35DMP, silver, or CD. The purified precipitate was dried under vacuum at room temperature and stored in an airtight container. The resulting powdered samples were used for subsequent analyses [24-28].

3. Results and Discussion

3.1. Effect of α-CD and β-CD on 3,5-Dimethylphenol at Different pH

The absorption and fluorescence maxima of 3,5-dimethylphenol (35DMP) (1×10^{-4} M) in buffer solutions of pH ~2, pH ~7, and pH ~11 at various α-CD and β-CD concentrations are presented in Table 1, Figure 1, and Figure 2. Since 35DMP exists predominantly as a monoanion in pH ~7 buffer, its inclusion behavior in both the neutral and hydroxyl-anion forms can be compared by studying the system across different pH conditions. In water, pH ~3, and pH ~7 solutions, the absorption maxima of 35DMP appear at 272–278 nm, whereas at pH ~11, three bands are observed at 290, 241, and 216 nm. In the absence and presence of α-CD or β-CD, the absorption and emission spectral profiles of 35DMP remain nearly identical in water, pH ~3, and pH ~7, but differ in pH ~11.

With increasing α-CD or β-CD concentration, no significant absorption shifts occur at pH ~3 or pH ~7. At pH ~11, α-CD causes no measurable shift, whereas β-CD induces a distinct blue shift from 290 to 272 nm. In both α-CD and β-CD media, a decrease in absorbance is observed at all three pH values. The change in absorbance upon CD addition confirms the formation of 35DMP: CD inclusion complexes [16-30]. At higher CD concentrations, the absorption maxima and spectral shapes at pH ~2 and pH ~7 become similar, suggesting that comparable inclusion modes are formed under these conditions.

Figure 2 illustrates the fluorescence spectra of 35DMP at pH ~2, pH ~7, and pH ~11 in the presence of varying concentrations of α-CD and β-CD. The influence of β-CD on the fluorescence spectra is more pronounced than that of α-CD. In water and in CD solutions at pH ~3 and pH ~7, the emission maxima remain unchanged, whereas they differ significantly at pH ~11. In α-CD solutions, the emission maximum appears at 299 nm at pH ~3 and pH ~7, and at 308 nm at pH ~11. At all pH values, increasing α-CD concentration enhances fluorescence intensity, while increasing β-CD concentration results in decreased intensity at the same wavelengths. A red shift of the emission maximum (299 → 305 nm) occurs in pH ~3 and pH ~7, whereas a blue shift (308 → 303 nm) is observed at pH ~11.

In all pH conditions, the presence of an isosbestic point in the absorption spectra indicates formation of a 1: 1 inclusion complex between 35DMP and the CDs [16-30]. However, in α-CD, the absorption and fluorescence spectra at pH ~2 and pH ~7 differ markedly from those at pH ~11, suggesting the existence of at least two distinct types of inclusion complexes. Binding constants for the 35DMP–CD systems were calculated using the Benesi–Hildebrand method. The negative values of ΔG indicate that the inclusion process is spontaneous and exothermic at 303 K [16-30].

Table 1. *Absorption and fluorescence maxima and lifetime of 3,5-dimethylphenol (35DMP) with different α-CD and β-CD concentrations.*

Concentration of α-CD x10^{-3} M	**pH -3**				**pH - 7**				**pH - 11**			
	λ_{abs}	**log ε**	**λ_{flu}**	**τ**	**λ_{abs}**	**log ε**	**λ_{flu}**	**τ**	**λ_{abs}**	**log ε**	**λ_{flu}**	**τ**
35DMP only (without CD)	272-278 210	3.49	299	0.36	272-278	3.43	299	0.36	290 241 216	3.52	308	0.23
0.2 M α-CD	272-278 213	3.42	299	0.43	272-278	3.44	299	0.45	290 241 216	3.50	308	0.38
1.0 M α-CD	272-278 221	3.40	299	0.46	272-278	3.48	299	0.48	290 241 216	3.43	308	0.42
0.2 M β-CD	272-278 213	3.39	300	0.48	272-278	3.47	300	0.51	272-279 213	3.47	303	0.44
1.0 M β-CD	272-278 221	3.23	305	0.56	272-278	3.37	305	0.63	272-278 221	3.36	304	0.58
K (1: 1) x10^{5} M^{-1} α-CD	81.1		289		74.4		355		82.2		223	
ΔG (kcalmol^{-1}) α-CD	-11.08		-14.27		-10.85		-14.79		-11.08		-13.62	
K (1: 1) x10^{5} M^{-1} β-CD	122.2		337		129.2		793		125		793	
ΔG (kcalmol^{-1}) β-CD	-12.0		-14.9		-12.2		-16.8		-12.1		-16.8	
Excitation wavelength (nm)				270			270				270	

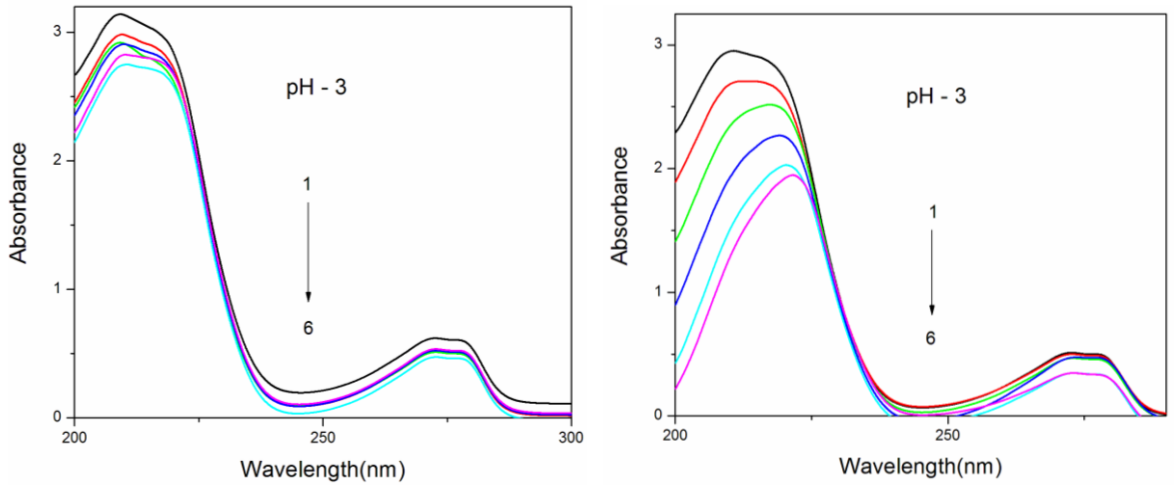

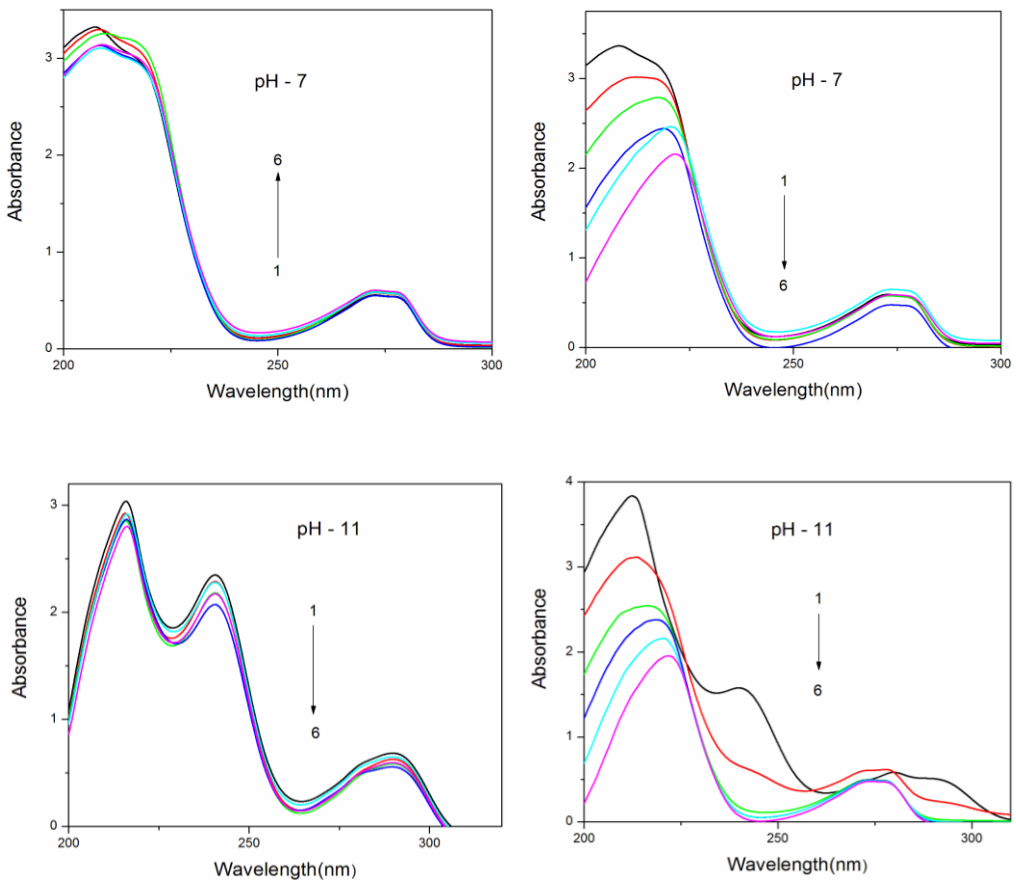

Figure 1. *Absorbance spectra of 35-DMP in different α-CD and β-CD concentrations (M): (1) 0, (2) 0.002, (3) 0.004, (4) 0.006, (5) 0.008 and (6) 0.01.*

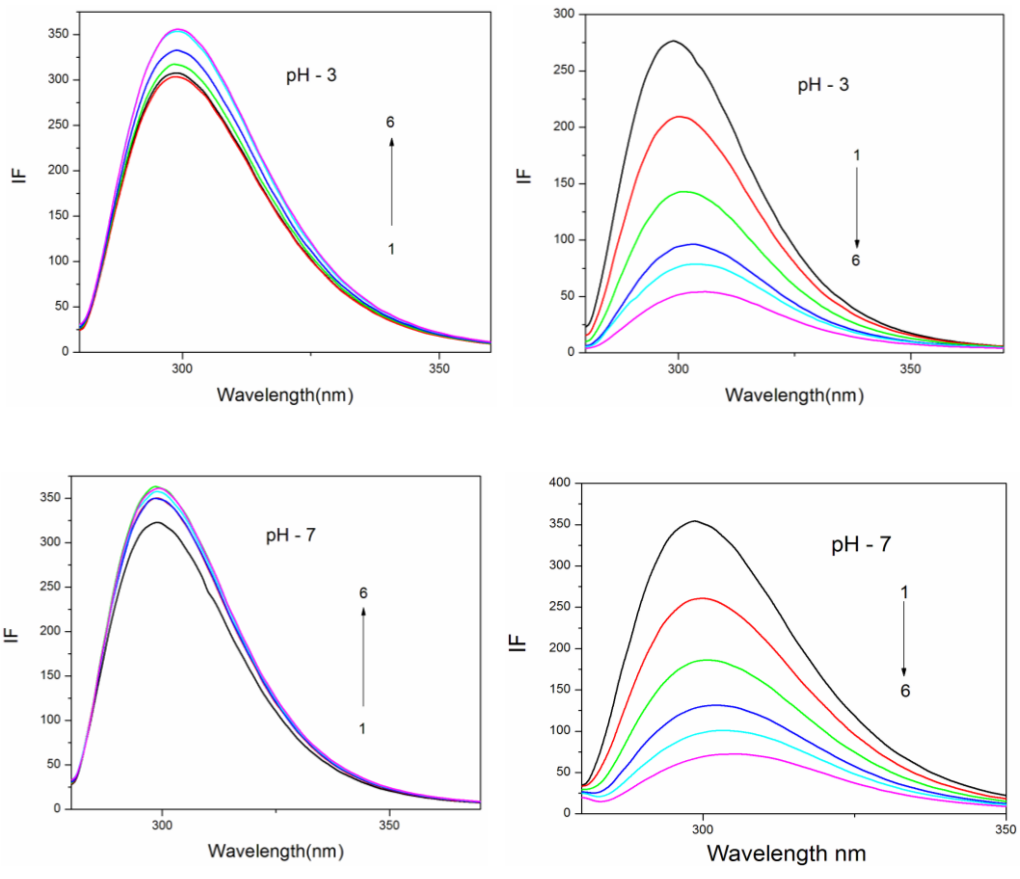

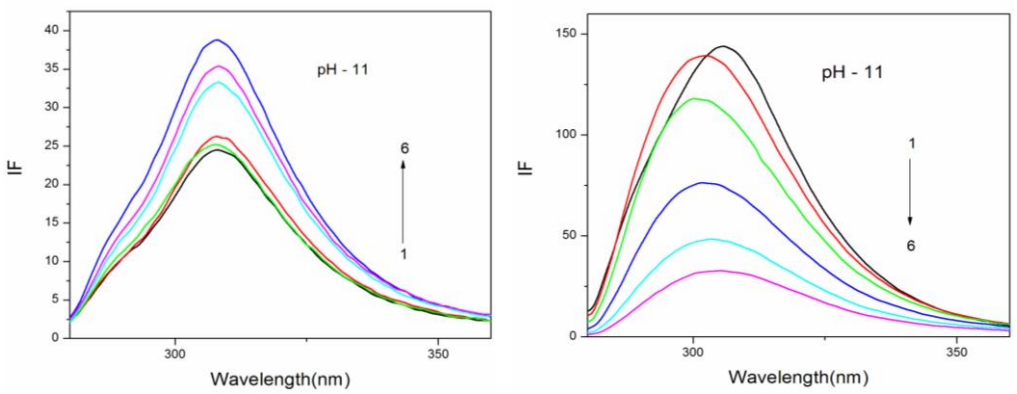

Figure 2. *Fluorescence spectra of 35-DMP in different α-CD and β-CD concentrations (M): (1) 0, (2) 0.002, (3) 0.004, (4) 0.006, (5) 0.008 and (6) 0.01.*

It is well established that the strength of host–guest interactions depend on both the size of the cyclodextrin cavity and the dimensions of the guest molecule [16-30]. Consequently, the complexation process is highly sensitive to the substituent size on the guest and the type of CD employed. Van der Waals forces, including dipole–induced dipole interactions, are directly related to the distance between the guest molecule and the CD cavity wall, as well as to the polarizabilities of both components. Thus, the neutral 35DMP molecule is expected to penetrate more deeply into the β-CD cavity than into α-CD. The phenyl ring of 35DMP likely attains greater contact with the inner surface of β-CD, and this interaction is a major factor governing the inclusion process.

To validate the inclusion behavior, the spectral properties of 35DMP: CD complexes were compared with those of phenol in different solvents. Relative to phenol [29-32] which exhibits $\lambda_{\_abs} \approx 271–277$ nm and $\lambda_{emi} \approx 300$ nm in cyclohexane; $\lambda_{abs} \approx 272–278$ nm and $\lambda_{emi} \approx 305$ nm in acetonitrile; $\lambda_{abs} \approx 272–275$ nm and $\lambda_{emi} \approx 305$ nm in methanol; and $\lambda_{abs} \approx 269$ nm and $\lambda_{emi} \approx 305$ nm in water (pH ~2) 35DMP shows slightly blue-shifted emission in all solvents (cyclohexane: $\lambda_{emi} \approx 298$ nm; acetonitrile: $\lambda_{emi} \approx 298$ nm; methanol: $\lambda_{emi} \approx 299$ nm; water (pH ~2): $\lambda_{emi} \approx 300$ nm), while the absorption maxima remain similar (272–278 nm).

Solvatochromic analysis shows negligible absorption shifts for 35DMP, whereas a modest blue shift is observed in the excited state. The spectral trends in various protic and aprotic solvents are consistent with the typical behavior of hydroxyl-containing aromatic systems [29-32]. In both α-CD and β-CD solutions, the absorption and emission maxima of 35DMP closely resemble those of phenol, indicating that substitution with two methyl groups does not significantly alter the conjugation of the aromatic ring. The broad absorption bands in both phenol and 35DMP point to the presence of intermolecular hydrogen bonding.

As noted earlier, increasing α-CD concentration leads to a decrease in absorbance at the same wavelength but results in enhanced fluorescence intensity across all pH values. In β-CD, absorbance decreases similarly at pH ~3 and pH ~7, while a notable blue shift is observed at pH ~11. Fluorescence intensities, however, decrease at all pH values in β-CD. Additionally, emission exhibits a red shift at pH ~3 and pH ~7, whereas a blue shift occurs at pH ~11. Remarkably, at high β-CD concentrations, the emission maximum converges to 305 nm at all three pH values. At elevated α-CD and β-CD concentrations, the differences in absorption and emission maxima and in the overall spectral profiles across the pH conditions indicate the formation of distinct types of inclusion complexes.

The 35DMP molecule is more deeply encapsulated within the β-CD cavity than within the α-CD cavity, owing to the larger internal diameter of β-CD. Because dipole–dipole interactions between 35DMP and the CD cavity wall are weakened in the less polar, hydrophobic interior, corresponding increases or decreases in absorption and emission intensities are observed [16-30]. In β-CD, both the absorption and emission maxima exhibit a consistent blue shift at pH ~11, indicating protonation of the hydroxyl monoanion. As CDs are known to act as effective proton donors, the β-CD cavity is capable of providing a proton to the entrapped hydroxyl anion.

The differences in the inclusion modes of α-CD and β-CD also account for the variations in their binding constants. The larger binding constants observed at pH ~2 and pH ~7 suggest that 35DMP is more tightly embedded in the CD cavity under these conditions than at pH ~11. In other words, the molecule is more effectively entrapped in the nonpolar region of β-CD than in α-CD. This is consistent with the fact that the distance between the two methyl substituents in 35DMP is greater than the interior cavity size of α-CD but smaller than that of β-CD. Accordingly, fluorescence intensity increases progressively with α-CD concentration, whereas it decreases steadily with β-CD, in agreement with the proposed inclusion geometries.

We have previously reported that when carboxyl or hydroxyl groups are deeply embedded within the nonpolar CD cavity, the absorption and emission maxima undergo red or blue shifts relative to aqueous solution, reflecting the cyclohexane-like hydrophobicity of the cavity interior [16-30]. Furthermore, if the hydroxyl anion resides in the hydrophilic region of the cavity, protonation is expected to occur. Under such circumstances, a blue shift in spectral maxima should be

observed, and the absorption and emission wavelengths should resemble those seen at pH ~3 and pH ~7, where the neutral species predominates. As shown in Table 1, the absorption and emission maxima of the monoanion are similar to those in aqueous solution when α-CD is present, but are blue shifted in β-CD. These results demonstrate that in the 35DMP–β-CD system, the hydroxyl group is located within the hydrophobic interior of the cavity, whereas in α-CD, it resides in the more hydrophilic region.

3.2. Excited Singlet State Lifetimes

The formation of the inclusion complex was further investigated using fluorescence decay profiles recorded for both α-CD and β-CD. Fluorescence lifetimes of 35DMP in aqueous and CD media were obtained from these decay curves (Table 1). The lifetimes of the 35DMP: CD complexes were longer than that of free 35DMP, which can be attributed to restricted vibrational relaxation of the encapsulated molecule in the excited state. The progressive increase in lifetime with increasing CD concentration reflects the enhanced encapsulation of 35DMP within the CD cavity. Notably, the lifetime of the 35DMP: β-CD complex is longer than that of 35DMP: α-CD, indicating deeper penetration of the guest into the β-CD cavity. These findings collectively demonstrate the stronger complexation capability of β-CD compared to α-CD.

3.3. Molecular Modeling

The ground-state geometries of 35DMP and the CDs were optimized using the PM3 method (Table 2 and Figure 3). The calculated HOMO and LUMO energies, dipole moments, total energies, free energies, enthalpies, entropies, and zero-point vibrational energies of pure 35DMP, α-CD, and β-CD differ from those of their corresponding inclusion complexes. For 35DMP, the vertical and horizontal distances between the OH and CH_3 groups are 5.70 Å and 6.64 Å, respectively (Figure 3). Both CDs have the same height (7.8 Å), but their internal cavity diameters differ: 4.7–5.3 Å for α-CD and 6.0–6.5 Å for β-CD. The exterior diameters are 8.8 Å for α-CD and 10.8 Å for β-CD. The vertical bond length of 35DMP is smaller than the inner cavity dimensions of both CDs, while the horizontal bond length exceeds the α-CD cavity size but fits within that of β-CD. Thus, the distance between the two methyl groups in 35DMP is too large for full accommodation in α-CD but compatible with the β-CD cavity. Considering these geometric factors, 35DMP can be encapsulated in both CDs, though with different modes of inclusion. These results support the conclusion that the encapsulation geometry of 35DMP differs between α-CD and β-CD.

Table 3 data show that the geometry of 35DMP undergoes slight modifications upon complexation, with the most notable changes occurring in the dihedral angles. These variations indicate that 35DMP adopts a specific conformation to achieve stable binding within the CD cavity. The optimized structures of the CD: 35DMP complexes confirm successful inclusion of the guest molecule. Additionally, the Mulliken charges of the complexes are approximately zero, indicating the absence of charge-transfer interactions between host and guest. The thermodynamic parameters (ΔE, ΔG, and ΔH) further reveal that the complexation of 35DMP with CDs is predominantly enthalpy-driven and energetically favorable.

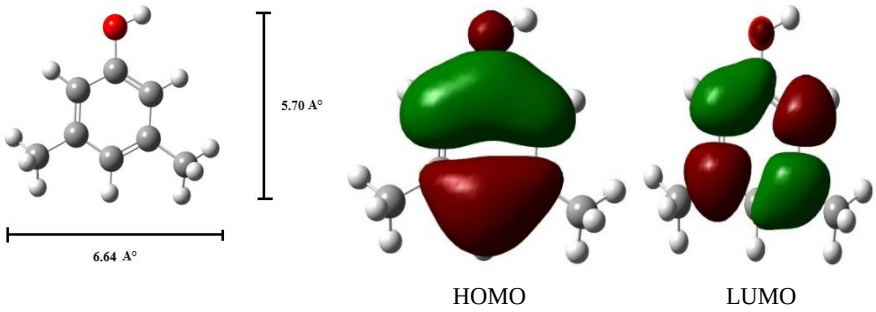

Figure 3. *PM3 optimized structures of (a, b) 35DMP, (c, d) HOMO, LUMO of 35DMP.*

Table 2. ***T****hermodynamic parameters and HOMO-LUMO energy calculations for 35DMP and its inclusion complexes by PM3 method.*

Properties	35DMP	α-CD	β-CD	35DMP: α-CD	35DMP: β-CD
E_{HOMO} (eV)	-8.93	-10.37	-10.35	-8.51	-8.55
E_{LUMO} (eV)	0.44	1.26	1.23	0.74	-0.79
$E_{HOMO} – E_{LUMO}$ (eV)	-9.37	-11.63	-11.58	-9.25	-9.34
Dipole moment (D)	1.74	11.34	12.29	11.61	11.83

Properties	35DMP	α-CD	β-CD	35DMP: α-CD	35DMP: β-CD
E*	-42.62	-1247.62	-1457.63	-1283.97	-1459.81
ΔE*	-	-	-	-3.73	-59.58
G*	71.21	-676.37	-789.52	-635.83	-689.52
ΔG*	-	-	-	-30.67	-71.21
H*	96.86	-570.84	-667.55	-540.76	-641.18
ΔH	-	-	-	-66.78	-70.49
S**	0.085	0.353	0.409	0.418	0.484
ΔS**	-	-	-	-0.02	-0.01
ZPE*	69.45	635.09	740.56	746.37	812.19
Mullikan charge	0.00	0.00	0.00	0.00	0.00

* kcal/mol; **kcal/mol-Kelvin; ZPE = Zero point vibration energy

3.4. Nanomaterial Studies

3.4.1. Scanning Electron Microscopy

The powdered forms of Ag nanoparticles, 35DMP, and the Ag: 35DMP: α-CD and Ag: 35DMP: β-CD inclusion complexes were examined using SEM (Figure 4). The images clearly show that the Ag nanoparticles form clustered spherical structures, 35DMP appears as irregular stone-like particles, while nanorod-like structures are observed in the Ag: 35DMP: α-CD and Ag: 35DMP: β-CD nanomaterials. SEM-EDX analysis confirmed the elemental composition of the nanomaterials as 38.49% carbon, 49.57% oxygen, and 11.95% silver. The observed morphological changes provide strong evidence for the successful formation of the nanomaterials and highlight the structural differences between pure Ag nanoparticles, 35DMP, and the Ag: 35DMP: CD complexes.

3.4.2. Differential Scanning Colorimeter

The DSC thermograms of the CDs show characteristic endothermic peaks due to loss of crystallization water. β-CD exhibits a broad endothermic peak at 128.6°C, whereas α-CD shows three endothermic peaks at 79.2 ℃, 109.1 ℃, and 137.5 ℃. Pure 35DMP shows a sharp endothermic peak at 66 ℃, corresponding to its melting point. The DSC curves of α-CD, β-CD, and their respective nanomaterials show broader endothermic effects, attributed to water loss from the CD cavities [33-42]. In contrast, the nanomaterials (Ag: 35DMP: α-CD and Ag: 35DMP: β-CD) display new endothermic peaks at 251 ℃ and 267 ℃, respectively, with no peaks corresponding to pure 35DMP or CDs, confirming the formation of new inclusion complexes.

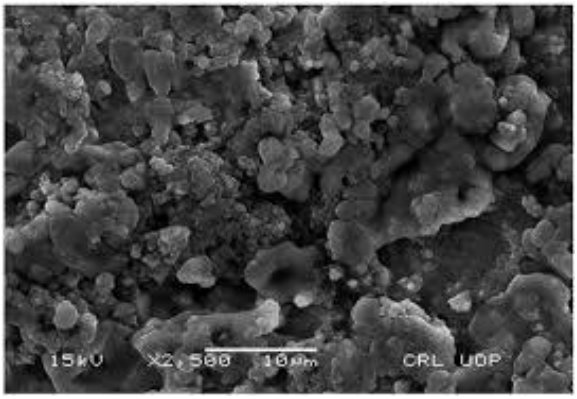

a) Ag nano

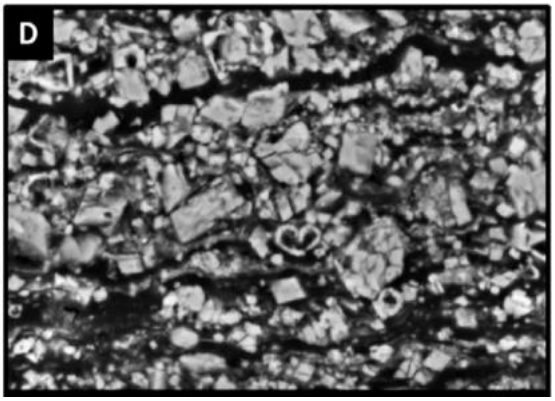

b) 35DMP

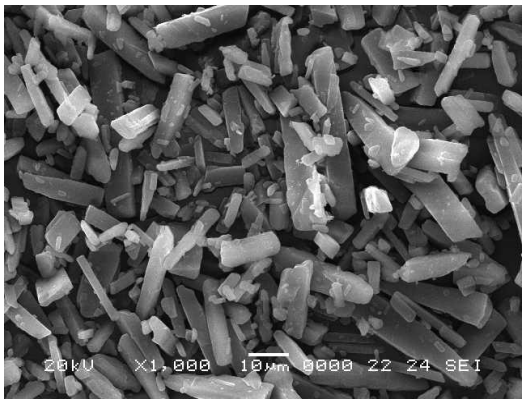

c) Ag: 35DMP: α-CD

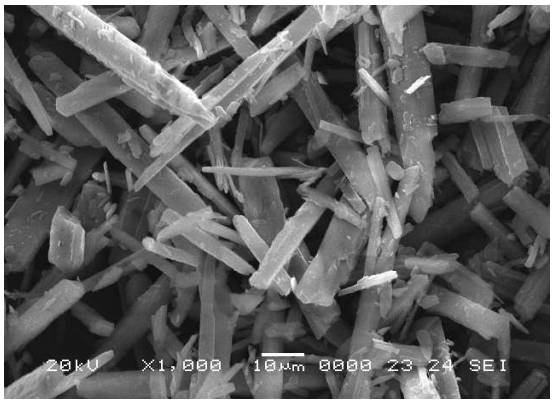

d) Ag: 35DMP: β-CD

Figure 4. *SEM images for a) Ag nano, b) 35DMP, c) Ag: 35DMP: α-CD and d) Ag: 35DMP: β-CD.*

3.4.3. Infrared Spectral Studies

FTIR spectra of pure 35DMP, α-CD, β-CD, and Ag: 35DMP: CD nanomaterials were analyzed to investigate molecular interactions. In 35DMP, the –OH stretching vibration appears at 3297 cm^{-1} and the out-of-plane –OH bending is observed at 686 cm^{-1}. Aromatic C–H, C–C, and C=C stretching vibrations appear at 3038 cm^{-1}, 1595 cm^{-1}, and 1443 cm^{-1}, respectively. The C–CH_3 stretching frequencies appear at 2976–2855 cm^{-1}, with CH_3 deformation at 1379 cm^{-1}, and C–H bending at 850 and 686 cm^{-1}.

In the Ag: 35DMP: CD nanomaterials, the –OH stretching shifts to 3294 cm^{-1}, aromatic C–H and C=C stretching appear at 2878 cm^{-1} and 1632 cm^{-1}, respectively. The C–O stretching vibrations at 1347 and 1155 cm^{-1} in 35DMP shift to 1303 and 1003 cm^{-1} in the nanomaterials, while the Ar–OH bending at 581 and 575 cm^{-1} moves to 561 cm^{-1}. Many characteristic 35DMP peaks are absent or significantly reduced in intensity in the nanomaterials, indicating strong interactions between 35DMP, silver nanoparticles, and the CD cavity.

3.4.4. XRD Spectral Studies

The crystallinity of all nanoparticles was examined using XRD analysis [33-42]. Pure Ag nanoparticles exhibited strong diffraction peaks at 38.11 °, 44.30 °, 64.45 °, and 77.40 °, corresponding to the (111), (200), (220), and (311) planes of the face-centered cubic structure of metallic silver. The XRD pattern of α-CD revealed crystalline peaks at approximately 11.94°, 14.11°, and 21.77°, while β-CD displayed peaks at 11.49 °and 17.58 °, with intensities varying depending on sample preparation. 35DMP showed an orthorhombic system with characteristic peaks at 8.24 °, 11.52 °, 22.55 °, and 83.77 °. The Ag: 35DMP: β-CD nanomaterials exhibited distinct diffraction peaks at 11.13 °, 18.24 °, 26.75 °, 33.56 °, 44.82 °, 68.14 °, and 76.77 °. The differences in peak positions and intensities between the nanomaterials and the pure components indicate the formation of new nanostructured materials.

3.4.5. ^{1}H-NMR Spectral Studies

^{1}H-NMR spectra of pure 35DMP and the inclusion complexes were recorded at 25 ℃ in DMSO-d_6, and the chemical shift data are summarized in Table 3. The chemical shifts of the aromatic protons in the Ag: 35DMP: CD nanomaterials shifted upfield relative to free 35DMP, indicating interactions between these protons and the CD cavity. The hydroxy proton also exhibited a higher chemical shift, suggesting hydrogen bonding with CD hydroxyl protons. Additionally, the aromatic protons are more upfield shifted than the methyl protons, implying that the aromatic ring is largely shielded and deeply embedded within the CD cavity and in proximity to the silver nanoparticles.

4. Conclusion

The absorption and fluorescence behavior of 3,5-dimethylphenol (35DMP) was investigated in varying concentrations of α-CD and β-CD at pH ~2, pH ~7, and pH ~11. In CD solutions, the absorption and emission spectra of 35DMP are similar at pH ~2 and pH ~7 but differ at pH ~11. At higher β-CD concentrations, the spectral maxima and shapes are consistent across all pH values, suggesting the formation of a uniform type of inclusion complex. In contrast, α-CD shows distinct absorption and emission maxima at different pH values, indicating the formation of multiple inclusion modes. 35DMP is more deeply encapsulated in the nonpolar interior of β-CD than in α-CD, as reflected by the increase in fluorescence lifetime in the order: pH < α-CD < β-CD. SEM images reveal clear morphological differences between Ag nanoparticles, 35DMP, and the Ag: 35DMP: CD nanomaterials. SEM-EDX analysis confirmed the presence of 38.49% carbon, 49.57% oxygen, and 11.95% silver in the nanomaterials. DSC thermograms of Ag: 35DMP: CD complexes show new thermal peaks distinct from those of pure 35DMP, α-CD, and β-CD. FTIR spectra of the nanomaterials indicate substantial decreases or absence of most characteristic peaks, confirming

strong interactions between 35DMP, the CD cavity, and the silver nanoparticles.

Abbreviations

FTIR	Fourier Transform Infrared Spectroscopy
DTA	Differential Thermal Analysis
XRD	X-ray Diffraction
SEM	Scanning Electron Microscopy
HOMO	Highest Occupied Molecular Orbital
LUMO	Lowest Unoccupied Molecular Orbital
35DMP	3,5-dimethylphenol
Ag NPs	Silver Nanoparticles
α-CD	Alpha Cyclodextrin
β-CD	Beta Cyclodextrin
PM3	Parametric Method 3
ΔE	Iinternal Energy Change
ΔH	Enthalpy Change
ΔG	Free Energy Change
ΔS	Entropy Change

Author Contributions

Narayanasamy Rajendiran: Supervision, Resources, Methodology, Software, Writing – original draft, Writing – review & editing

Ayyadurai Mani: Formal Analysis, Investigation

Palanichamy Ramasamy: Data curation

Sengamalai Senthilmurugan: Validation

Conflicts of Interest

The authors declare no conflict of interest.

References

[1] K. Kalyanasundaram, *Photochemistry in Microheterogeneous Systems*, Academic Press, Orlando, FL (1987).

[2] S. Mitra, R. Das, S. Mukherjee, *Intramolecular Proton Transfer in Inclusion Complexes of Cyclodextrins: Role of Water and Highly Polar Nonaqueous Media*, J. Phys. Chem. B 102 (1998) 3730-35. https://doi.org/10.1021/jp980012l

[3] K. Kano, N. Tanaka, H. Minamizono, Y. Kawakita, *Tetraarylporphyrins as Probes for Studying Mechanism of Inclusion-Complex Formation of Cyclodextrins: Effect of Microscopic Environment on Inclusion of Ionic Guests*, Chem. Lett. (1996) 925=26. https://doi.org/10.1246/cl.1996.925

[4] Hiba Mohamed Ameen, S. Kunsági-Máté, L. Szente, B. Lemli, *Thermodynamic Characterization of the Complexation of Methyl Orange with β-Cyclodextrin Derivatives in Water, Cyclodextrin Chemistry and Toxicology* Spectrochim. Acta A 225 (2020) 117475. https://doi.org/10.1016/j.saa.2019.117475

[5] Marzena Jamróg̨iewicz, Karolina Milewska, *Studies on the Influence of β-Cyclodextrin Derivatives on the Physical Stability of Famotidine*, Spectrochim. Acta A 219 (2019) 346-357. https://doi.org/10.1016/j.saa.2019.04.047

[6] Maryam Akhondi, Effat Jamalizadeh, Ali Mohebbi, *MD and DFT Calculations on the Structural Variations of Amino-Cyclodextrin as a pH-Sensitive Carrier for Smart Carriage and Release of Doxorubicin*, J. Mol. Struct. 1230 (2021) 129855. https://doi.org/10.1016/j.molstruc.2020.129855

[7] Lafifi Ismahan, Nouar Leila, Madi Fatiha, Guendouzi Abdelkrim, Cheriet Mouna, Boulaha Nada, Houari Brahim, *Exploring the Inclusion Complex of a Drug (Umbelliferone) with β-Cyclodextrin by Spectro-Electrochemical and Computational Approaches*, J. Mol. Struct. 1206 (2020) 127740. https://doi.org/10.1016/j.molstruc.2019.127740

[8] H. E. Edwards, J. K. Thomas, *Pyrene inclusion by cyclomaltooligosaccharides. I. Steady-state and time-resolved fluorescence of pyrene with β-, γ- and mixed cyclodextrins*, Carbohydr. Res. 65(1978) 173-182. https://doi.org/10.1016/S0008-6215(00)82214-3

[9] Mohamad A. Chouker, Hiba Abdallah, Ali Zeiz, Mohammad H. El-Dakdouki, Synthesis, antibacterial and anticancer evaluation, DFT, molecular dynamics simulation and molecular docking studies of new benzimidazole-pyrazole derivatives, J. Mol. Struct. 1235 (2021) 130273. https://doi.org/10.1016/j.molstruc.2021.130273

[10] S. K. Das, Inclusion complexation of 2-(4′-N,N-dimethylaminophenyl)-1H-naphth [2,3-d] imidazole by β-cyclodextrin: effect on the twisted intramolecular charge transfer emission, Chem. Phys. Lett. 361 (2002) 21-28. https://doi.org/10.1016/S0009-2614(02)00876-4

[11] Asma Obaid, Arniza Khairani, Mohd Jamil, Samikannu Prabu, Siti Munirah Saharin, Sharifah Mohamad, Investigation of structural, spectroscopic and antioxidant properties of a new cyclodextrin-metal complex, Spectrochim. Acta A 225 (2020) 118674. https://doi.org/10.1016/j.saa.2019.118674

[12] 12. Mindy Levine, Benjamin R. Smith, Fluorescence lifetime imaging of cyclodextrin-based nanoprobes in live cells, J. Fluoresc. 30(2020) 1015-1023. https://doi.org/10.1007/s10895-020-02544-3

[13] Hui He, Chuchu Xie, Liu Yao, Ge Ning, Yonghong Wang, A novel β-cyclodextrin functionalized fluorescent probe for selective detection of metal ions in aqueous solution, J. Fluoresc. 31(2021) 63-71. https://doi.org/10.1007/s10895-020-02652-0

[14] N. Rajendiran, G. Venkatesh, Inclusion complexation of 4,4'-dihydroxy benzophenone and 4-hydroxy benzophenone with α- and β-CD. *Supramolecular Chemistry*, 26(2014) 783-795, https://doi.org/10.1080/10610278.2014.940911

[15] Gu Alice, Wheate Nial, Macrocycles as drug-enhancing excipients in pharmaceutical formulations, J. Incl. Phenom. Macrocycl. Chem. 100(2021) 55-69. https://doi.org/10.1007/s10847-021-01055-9

[16] J. Prema Kumari, A. Antony Muthu Prabhu, G. Venkatesh, V. K. Subramanian, N. Rajendiran, Effect of solvents and pH on β-CD Inclusion complexation of 2,4-dihydroxy azobenzene and 4-hydroxy azobenzene. *J. Solution Chemistry*, 40(2011) 327-347. https://doi.org/10.1007/s10953-010-9639-1

[17] J. Prema Kumari, A. Antony Muthu Prabhu, G. Venkatesh, V. K. Subramanian, N. Rajendiran, Spectral characteristics of sulfadiazine, sulfisomidine: Effect of solvents, pH and β-CD. *Physics and Chemistry of Liquids*, 49(2011) 108-132. https://doi.org/10.1080/00319104.2010.509724

[18] N. Rajendiran, S. Siva, J. Saravanan, Inclusion complexation of sulfa pyridine with α- and β-CDs: Spectral and molecular modeling study. *J. Molecular Structure*,1054-1055 (2013) 215-222. https://doi.org/10.1016/j.molstruc.2013.09.035

[19] N. Rajendiran, R. K. Sankaranarayanan, Azo dye/Cyclodextrin: New findings of identical nanorods through 2: 2 inclusion complexes. *Carbohydrate Polymers*, 106(2014) 422-431. https://doi.org/10.1016/j.carbpol.2014.01.030

[20] N. Rajendiran, R. K. Sankaranarayanan, J. Saravanan, A study of supramolecular host-guest interaction of dothiepin and doxepin drugs with cyclodextrin macrocycles. *J Molecular Structure*, 1067(2014) 252-260. https://doi.org/10.1016/j.molstruc.2014.03.051

[21] A. Antony Muthu Prabhu, N. Rajendiran, Encapsulation of labetalol, and pseudoephedrine in β-CD cavity: Spectral and molecular modeling studies. *J. Fluorescence*, 22(2012) 1461-1474. https://doi.org/10.1007/s10895-012-1083-8

[22] N. Rajendiran, G. Venkatesh, J.Saravanan, Supramolecular aggregates formed by sulfadiazine and sulfisomidine inclusion complexes with α- and β-cyclodextrin. Spectrochimica Acta, 129A (2014) 157-162, https://doi.org/10.1016/j.saa.2014.03.028

[23] N. Rajendiran, G. Venkatesh, T. Mohandoss, Fabrication of 2D nano sheet through self assembly behavior of sulfamethoxy pyridazine inclusion complex with α- and β-cyclodextrins. Spectrochim Acta A,123A (2014) 158-166, https://doi.org/10.1016/j.saa.2013.12.053

[24] A. Mani, P. Ramasamy, A. Antony Muthu Prabhu, N. Rajendiran, Investigation of Ag and Ag/Co bimetallic nanoparticles with naproxen-cyclodextrin inclusion complex. J. Molecular Structure, 1284 (2023) 135301-10. https://doi.org/10.1016/j.molstruc.2023.135301

[25] A. Mani, G. Venkatesh, P. Senthilraja, N. Rajendiran, Synthesis and Characterisation of Ag-Co-Venlafaxine-Cyclodextrin Nanorods, European J Advanced Chemistry Research, 5(2024) 9-16. https://doi.org/10.24018/ejchem.2024.5.1.147

[26] A. Mani, P. Ramasamy, A. Antony Muthu Prabhu, P. Senthilraja, N. Rajendiran, Synthesis and Analysis of Ag/Olanzapine /Cyclodextrin and Ag/Co/Olanzapine /Cyclodextrin Inclusion Complex Nanorods. Physics and Chemistry of Liquids, 62(2024) 196-209. https://doi.org/10.1080/00319104.2023.2297223

[27] A. Mani, P. Ramasamy, A. Antony Muthu Prabhu, P. Senthilraja, N. Rajendiran, Synthesis and Characterisation of Ag/Co/Chloroquine/Cyclodextrin Inclusion Complex Nanomaterials. J Sol-Gel Science and Technology 115 (2025) 844-856. https://doi.org/10.1007/s10971-024-06620-5

[28] N. Rajendiran, A. Mani, M. Venkatesan, B. Sneha, E. Nivetha, P. Senthilraja, Spectral, Microscopic, Antibacterial and Anticancer Activity of Pyrimethamine drug with Ag nano, DNA, RNA, BSA, Dendrimer, and Cyclodextrins, J Solution Chem, https://doi.org/10.1007/s10953-025-01529-1

[29] T. Stalin, P. Vasantharani, B. Shanthi, A. Sekar, N. Rajendiran, Inclusion complex of 1,2,3-trihydroxybenzene with α- and β-cyclodextrins. *Indian J Chemistry*, 45A (2006) 1113-1120.

[30] R. K. Sankaranarayanan, S. Siva, A. Antony Muthu Prabhu, N. Rajendiran, A study on the inclusion complexation of 3,4,5-trihydroxy benzoic acid with β-CD at different pH. *J.Inclusion Phenomena and Macrocyclic Chemistry*, 67(2010) 461-470. https://doi.org/10.1007/s10847-009-9729-0

[31] S. Siva, R. K. Sankaranarayanan, A. Antony Muthu Prabhu, N. Rajendiran, Inclusion complexation of 3,5-dihydroxy benzoic acid with β-CD at different pH. Indian J. Chemistry, 48A (2009)1515-1521.

[32] T. Stalin, R. Anithadevi, N. Rajendiran, Spectral characteristics of ortho, meta and para-dihydroxybenzenes in different solvents, pH and β-CD. *Spectrochimica Acta*, 61A (2005) 2495-2504. https://doi.org/10.1016/j.saa.2004.08.024

[33] P Ramasamy, A Mani, B Sneha, E Nivetha, M Venkatesan, N Rajendiran, Azo-hydrazo tautomerism in Sudan Red-B and Cyclodextrin/ Sudan Red-B doped ZnO nanomaterials. J Molecular Structure 1329 (2025) 141423-32. https://doi.org/10.1016/j.molstruc.2025.141423

[34] P. Ramasamy, A. Mani, B. Sneha, E. Nivetha, A. Antony Muthu Prabhu, G. Venkatesh, N. Rajendiran,* Synthesis and Characterisation of Sudan Red-G/Cyclodextrin doped ZnO Nanocrystals. American J Physical Chemistry 14(2025) 23-32, https://doi.org/10.11648/j.ajpc.20251402.12

[35] P. Ramasamy, A. Mani, B. Sneha, E. Nivetha, A. Antony Muthu Prabhu, G. Venkatesh, P. Senthilraja, N. Rajendiran*, Synthesis and Characterisation of Cyclodextrin /Methyl Violet doped ZnO Nanocrystals. Colloid and Surface Science 9(2025) 19-30, https://doi.org/10.11648/j.css.20250701.12

[36] P. Ramasamy, A. Mani, B. Sneha, E. Nivetha, A. Antony Muthu Prabhu, G. Venkatesh, P. Senthilraja, N. Rajendiran*, Synthesis and Characterisation of Cyclodextrin/ Sudan Black-B Caped ZnO/ Nanocrystals. American J Quantum Chemistry and Molecular Spectroscopy 9(2025) 1-11, https://doi.org/10.11648/j.ajqcms.20250901.11

[37] P. Ramasamy, A. Mani, A. Antony Muthu Prabhu, G. Venkatesh, N. Rajendiran* Azo-Imino Tautomerism in Sudan Red 7B/Cyclodextrin Coated ZnO Nanocomposites: Evidence by Spectral and Microscopic Perspectives. Science Journal of Chemistry 13(2025) 65 - 75, https://doi.org/10.11648/j.sjc.20251303.13

[38] P. Ramasamy, A. Mani, A. Antony Muthu Prabhu, G. Venkatesh, P. Senthilraja, N. Rajendiran* PICT Effects and Anticancer Potential on Rosaniline and Spectral Characterisation of Rosaniline/Cyclodextrin Covered ZnO/ Nanocrystals. International J. Pure and Applied Chemistry 26(2025) 107-121, https://doi.org/10.9734/irjpac/2025/v26i3921

[39] P. Ramasamy, A. Mani, P. Senthilraja, N. Rajendiran Keto-Enol Tautomerism and Anticancer Potential on Sudan Blue II and Synthesis and Characterisation of Sudan Blue II/ Cyclodextrin doped ZnO Nanocrystals, J. Materials Science and Nanotechnology, 13(2025) 1-16.

[40] P. Ramasamy, A. Mani, P. Senthilraja, N. Rajendiran, Spectral, Microscopic and Anticancer Activity Investigation on Dimethyl Yellow/Cyclodextrin Doped ZnO Nanocomposites Journal of Chemical and Pharmaceutical Sciences (JCHPS) 18(3) (2025) 33-43.

[41] P. Ramasamy, A. Mani, P. Senthilraja, N. Rajendiran, Spectral Characteristics of ZnO/Mordent Yellow 12/ Cyclodextrin Nanomaterials, J Chemical Health Risks, (JCHR) 15(2025) 542-553, www.jchr.org

[42] P. Ramasamy, A. Mani, P. Senthilraja, S. Senthilmurugan, N. Rajendiran, Spectral, Microscopic and Anticancer Activity of 1,8-Diaminonaphthalene Doped ZnO Nanocrystals, VVI-JOURNAL 14(2026) 135-147, https://vvijournal.com